geosciences

MDPI

Supplementary Material

Climate Variability Indices – A Guided Tour

Mateusz Norel [1,2], Michał Kałczyński [1,2], Iwona Pińskwar [1,*], Krzysztof Krawiec [2,3] and Zbigniew W. Kundzewicz [1]

[11] Institute for Agricultural and Forest Environment, Polish Academy of Sciences, 60-809 Poznan, Poland; iwona.pinskwar@isrl.poznan.pl (I.P.); kundzewicz@yahoo.com (Z.W.K.)
[2] Institute of Computing Science, Poznań University of Technology, 60-965 Poznan, Poland; mateusznorel@gmail.com (M.N.); kalczynski.michal@gmail.com (M.K.)
[3] Center for Artificial Intelligence and Machine Learning (CAMIL), 60-965 Poznan, Poland; krzysztof.krawiec@cs.put.poznan.pl
* Correspondence: iwona.pinskwar@isrl.poznan.pl

The purpose of this Supplementary Material is to extend the information delivered in the body of the paper, by providing complementary tables and graphic material related to time series and quasi-periodic behaviour of ENSO indices (Nino and SOI type) as well as NAO indices that were not included in the main text. Tables S1 and S2 provide a range of characteristics of full-blown *El Niño* and *La Niña* episodes, corresponding to the Nino 3.4 index. Tables S3 and S4 refer to positive and negative phases of NOA. Figures S1 through to S3 present time series of Nino indices: Nino 1 + 2, Nino 3, Nino 4, respectively. Figures S4–S10 present time series of the SOI indices: Equatorial SOI Eastern Pacific Index, Equatorial SOI Indonesia index, Equatorial SOI Index, SOI Anomaly Index and SOI Standardized Index from NOAA, SOI from CRU and SOI from BoM, respectively. Figure S11 represents the time series of ONI. Figures S12–S14, complementary to Figures S1–S3 illustrate quasi-periodic behaviour of Nino indices via the wavelet analysis. Similarly, Figures S15–S21, complementary to Figures S4–S10 illustrate quasi-periodic behaviour of SOI indices via the wavelet analysis. Figure S22, complementary to S11 represents quasi-periodic behaviour of ONI. Figures S23–S26 present time series of NAO indices: Hurrell Index, PC-based Hurrell Index, NAO Index from CRU, and NAO Index from NOAA, respectively. Finally, Figures S27–S29, complementary to Figures S23–S25 illustrate quasi-periodic behaviour of various NAO indices via the wavelet analysis.

The artwork in Supplementary Material (SM) complements the short set of figures included in the main paper, avoiding redundancy. Hence, some essential figures are presented only in the main paper and others – only in SM.

S1 Characteristics of blown *El Niño* and *La Niña* episodes, corresponding to the Nino 3.4 index

Table S1. Characterization of full-blown *El Niño* episodes in 1870–2019, based on data illustrated in Figure 2.

# of El Niño	Starting Month	Ending Month	Time Since The End of Last El Niño Episode (Months)	Duration of Episode (Months)	Maximum Value	Time at Maximum	Cumulative Sum
1	1877/04	1878/08	-	17	2.27	1878/02	22.70
2	1888/06	1889/06	118	13	1.75	1889/02	13.15
3	1896/09	1897/05	87	9	1.36	1897/02	8.81
4	1899/10	1901/02	29	17	1.30	1900/03	13.47
5	1902/07	1903/06	17	12	1.42	1903/01	12.47
6	1904/10	1906/06	16	21	1.12	1905/12	15.77
7	1914/08	1915/08	98	13	0.65	1915/06	7.06
8	1918/11	1919/10	39	12	1.26	1919/02	10.14
9	1923/11	1924/04	49	6	0.76	1924/01	3.84
10	1925/10	1926/09	18	12	1.32	1926/04	11.39
11	1930/09	1931/08	48	12	1.44	1931/03	12.59
12	1940/02	1940/08	102	7	0.98	1940/05	5.21
13	1940/11	1942/04	3	18	1.38	1941/04	17.06
14	1951/09	1952/03	113	7	0.77	1951/12	4.21
15	1957/07	1958/06	64	12	1.24	1958/03	10.00
16	1963/09	1964/03	63	7	0.84	1963/12	4.92
17	1965/08	1966/06	17	11	1.42	1965/12	11.04
18	1968/12	1969/06	30	7	0.81	1969/03	4.46
19	1969/10	1970/04	4	7	0.62	1970/01	3.67
20	1972/08	1973/05	28	10	1.72	1973/01	12.23
21	1976/11	1977/04	42	6	0.76	1977/01	3.82
22	1977/10	1978/04	6	7	0.85	1978/02	4.60
23	1982/07	1983/08	51	14	2.21	1983/02	19.24
24	1986/11	1988/03	39	17	1.40	1987/11	18.31
25	1991/07	1992/08	40	14	1.55	1992/04	13.38
26	1993/04	1993/09	8	6	0.68	1993/06	3.42
27	1994/10	1995/05	13	8	1.04	1995/02	6.20
28	1997/06	1998/06	25	13	2.31	1998/01	21.05
29	2002/08	2003/04	50	9	1.16	2003/01	7.83
30	2004/10	2005/04	18	7	0.68	2004/12	3.96
31	2009/09	2010/06	53	10	1.40	2010/03	9.70
32	2014/11	2016/07	53	21	2.40	2016/02	27.34
33	2018/11	2019/08	28	10	0.79	2019/02	6.59
34	2019/11	2020/04	3	6	0.58	2020/02	2.96

Table S2. Characterization of full-blown *La Niña* episodes in 1870-2019, based on data illustrated in Figure 2.

# of La Niña	Starting Month	Ending Month	Time Since The End of Last La Niña Episode (Months)	Duration of Episode (Months)	Maximum Value	Time at Maximum	Cumulative Sum
1	1870/05	1871/10	-	18	−1.04	1870/06	−12.96
2	1872/01	1876/09	3	57	−1.18	1874/12	−45.87
3	1878/12	1880/09	27	22	−0.98	1880/01	−14.54
4	1882/10	1883/04	25	7	−0.66	1883/01	−4.10
5	1886/06	1887/10	38	17	−1.23	1886/12	−15.72
6	1889/09	1891/03	23	19	−1.65	1890/02	−21.31
7	1892/04	1895/04	13	37	−1.35	1893/02	−36.57
8	1898/01	1899/05	33	17	−0.69	1899/03	−9.44
9	1903/11	1904/06	54	8	−0.83	1904/03	−5.47
10	1906/10	1907/08	28	11	−0.62	1907/01	−5.69
11	1908/07	1911/08	11	38	−1.13	1909/12	−30.97
12	1916/04	1917/06	56	15	−1.53	1917/01	−14.36
13	1924/07	1925/06	85	12	−0.83	1924/11	−8.24
14	1933/07	1934/07	97	13	−1.03	1934/02	−10.30
15	1938/07	1939/06	48	12	−0.80	1939/03	−7.76
16	1942/09	1943/07	39	11	−1.29	1943/02	−10.79
17	1945/03	1946/02	20	12	−0.74	1945/10	−7.38
18	1949/09	1951/05	43	21	−1.23	1950/03	−19.71
19	1954/07	1957/03	38	33	−1.52	1956/01	−31.87
20	1964/07	1965/04	88	10	−0.97	1964/12	−7.73
21	1968/01	1968/06	33	6	−0.60	1968/05	−3.12
22	1970/08	1972/03	26	20	−1.22	1971/04	−16.74
23	1973/07	1976/06	16	36	−1.87	1974/02	−38.24
24	1983/11	1986/06	89	32	−1.09	1985/03	−22.75
25	1988/06	1989/11	24	18	−1.91	1989/02	−21.55
26	1995/11	1996/05	72	7	−0.71	1996/02	−4.25
27	1998/09	2001/05	28	33	−1.51	2000/03	−31.32
28	2007/09	2008/08	76	12	−1.62	2008/02	−12.80
29	2010/08	2012/05	24	22	−1.62	2011/01	−20.81
30	2017/12	2018/05	67	6	−0.80	2018/03	−4.14

Table S3. Characterization of NAO positive episodes in 1950–2019, based on data illustrated in Figure 13.

# of Positive Phase	Starting Month	Ending Month	Time Since The End of Last Positive Phase Episode (Months)	Duration of Episode (Months)	Maximum Value	Time at Maximum	Cumulative Sum
1	1959/06	1959/12	-	7	0.596	1959/11	3.294
2	1967/06	1967/12	90	7	0.85	1967/10	4.144
3	1971/11	1973/03	47	17	0.67	1972/10	8.272
4	1976/03	1976/09	36	7	0.74	1976/06	3.604
5	1978/09	1979/01	24	5	0.986	1978/11	3.52
6	1982/11	1983/04	46	6	1.198	1983/01	5.342
7	1986/11	1987/03	43	5	0.59	1987/02	2.284
8	1989/02	1989/11	23	10	1.336	1989/05	8.418
9	1990/03	1990/08	4	6	0.952	1990/04	3.954
10	1990/10	1991/05	2	8	0.554	1990/10	3.552
11	1992/02	1992/09	9	8	1.326	1992/06	7.264
12	1993/12	1994/08	15	9	1.376	1994/03	7.934
13	1999/12	2000/06	64	7	1.066	2000/03	5.996
14	2002/03	2002/08	21	6	0.638	2002/05	3.184
15	2011/12	2012/05	112	6	1.348	2012/03	6.062
16	2015/01	2015/06	32	6	1.43	2015/04	6.466
17	2015/12	2016/05	6	6	1.282	2016/03	5.304
18	2017/01	2017/07	8	7	0.886	2017/04	3.304
19	2018/01	2019/04	6	16	1.648	2018/09	14.89

Table S4. Characterization of NAO negative episodes in 1950–2019, based on data illustrated in Figure 13.

# of Negative Phase	Starting Month	Ending Month	Time Since The End of Last Negative Phase Episode (Months)	Duration of Episode (Months)	Maximum Value	Time at Maximum	Cumulative Sum
1	1952/09	1953/06	-	10	−0.622	1952/12	−4.732
2	1957/06	1957/10	48	5	−0.982	1957/09	−3.222
3	1958/03	1958/11	5	9	−0.996	1958/09	−6.816
4	1963/01	1963/05	50	5	−1.236	1963/04	−4.358
5	1968/04	1969/05	59	14	−1.476	1969/01	−13.296
6	1970/12	1971/04	19	5	−0.788	1971/01	−3.392
7	1977/01	1977/09	69	9	−0.768	1977/01	−4.782
8	1980/08	1980/12	35	5	−0.828	1980/10	−3.666
9	1985/01	1985/05	49	5	−0.446	1985/02	−1.882
10	1993/07	1993/11	98	5	−1	1993/09	−3.616
11	1995/12	1996/05	25	6	−0.696	1996/03	−2.998
12	1998/06	1998/12	25	7	−1.308	1998/09	−6.07
13	2002/10	2003/02	46	5	−0.788	2003/01	−2.808
14	2006/09	2007/01	43	5	−0.85	2006/11	−3.304
15	2008/06	2008/11	17	6	−1.324	2008/08	−4.904
16	2009/10	2011/03	11	18	−1.324	2010/04	−16.574
17	2012/07	2013/03	16	9	−1.496	2012/10	−7.814
18	2016/07	2016/11	40	5	−0.846	2016/08	−3.09
19	2019/06	2019/11	31	6	−1.294	2019/09	−5.324

S2 Time series of ENSO indices (Nino and SOI indices)

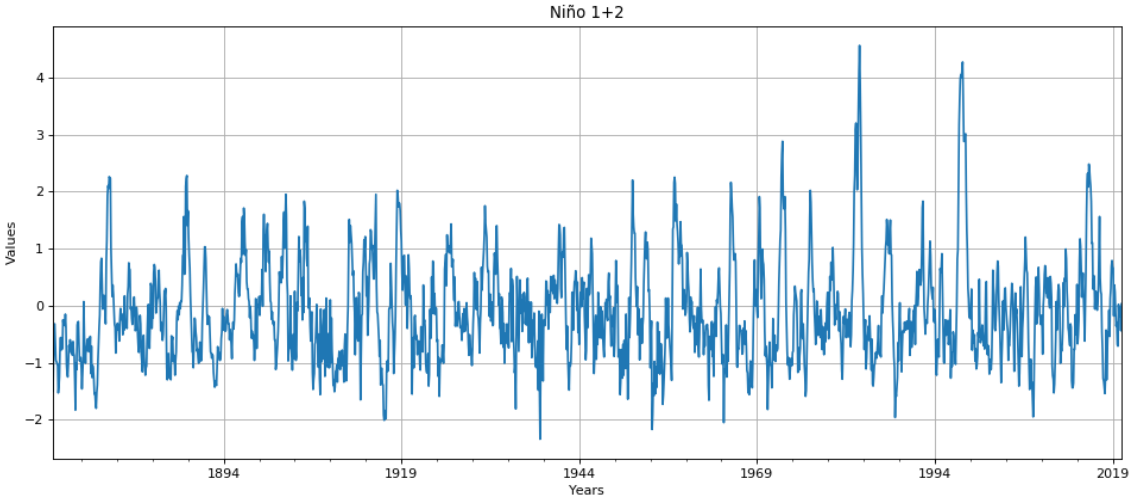

Figure S1. Time series of *Niño* 1 + 2 index, 1870–2019.

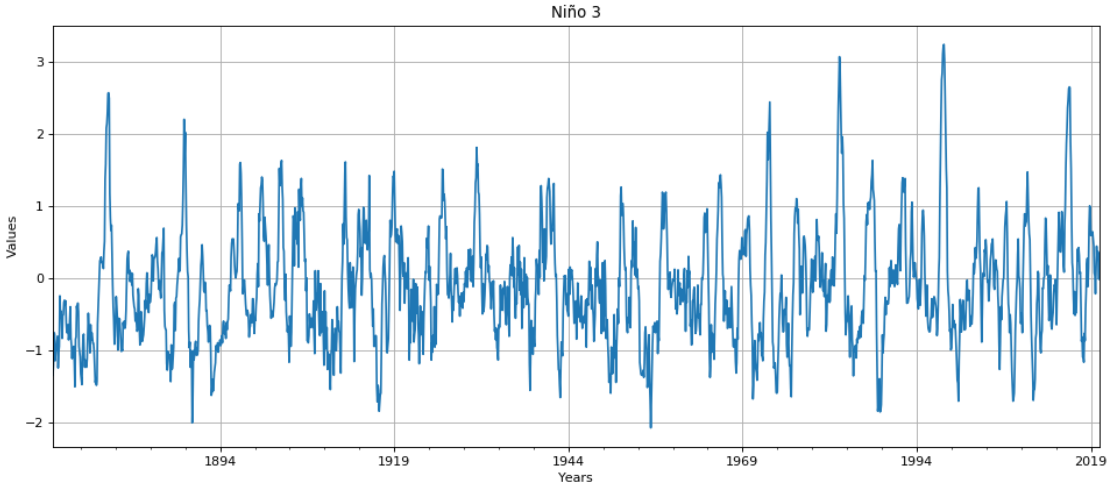

Figure S2. Time series of *Niño* 3 index, 1870–2019.

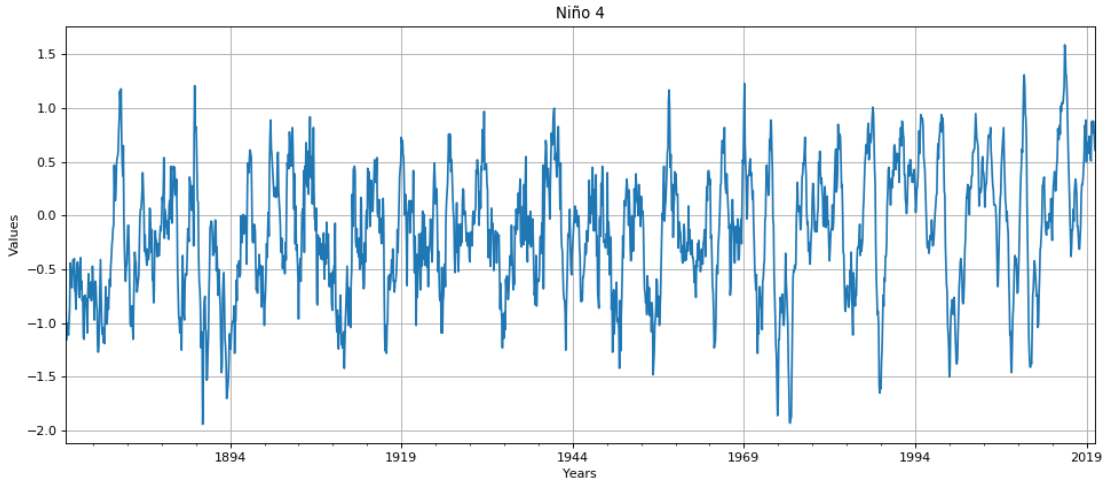

Figure S3. Time series of *Niño* 4 index, 1870–2019.

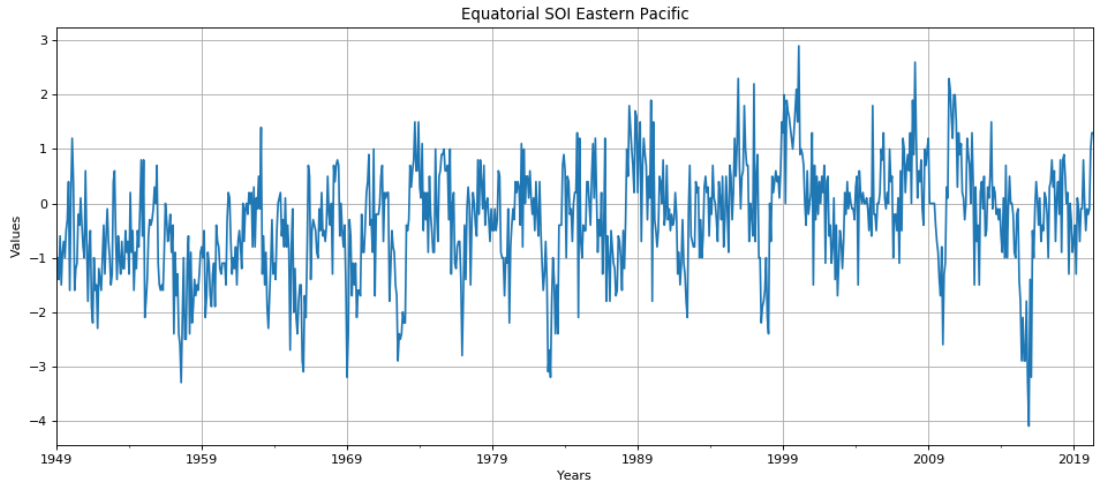

Figure S4. Time series of Equatorial SOI Eastern Pacific index, 1949–2019.

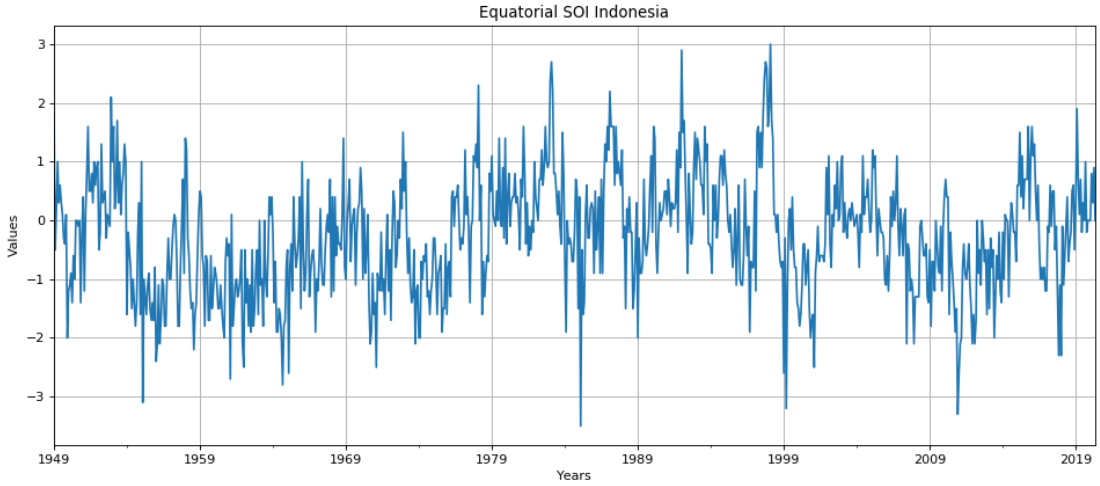

Figure S5. Time series of Equatorial SOI Indonesia index, 1949–2019.

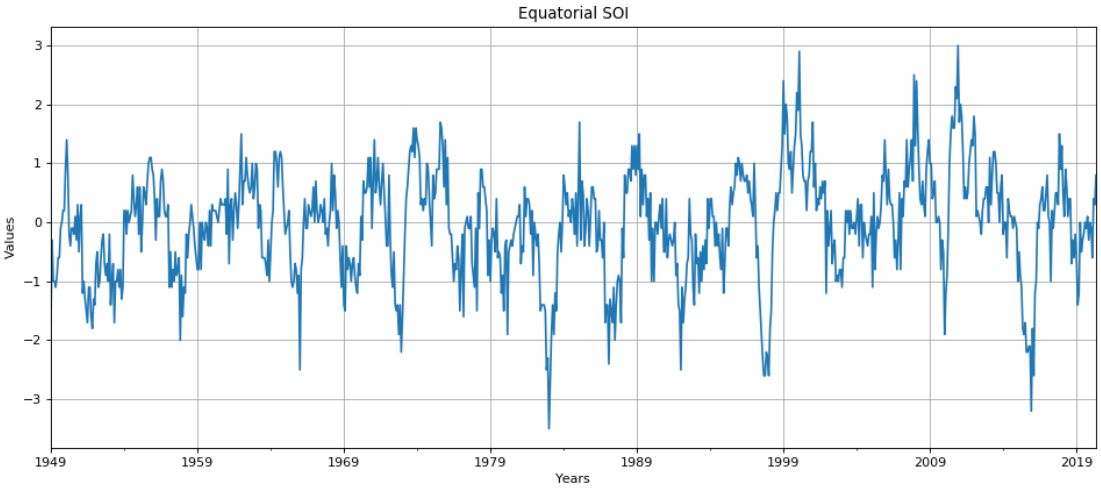

Figure S6. Time series of Equatorial SOI index, 1949–2019.

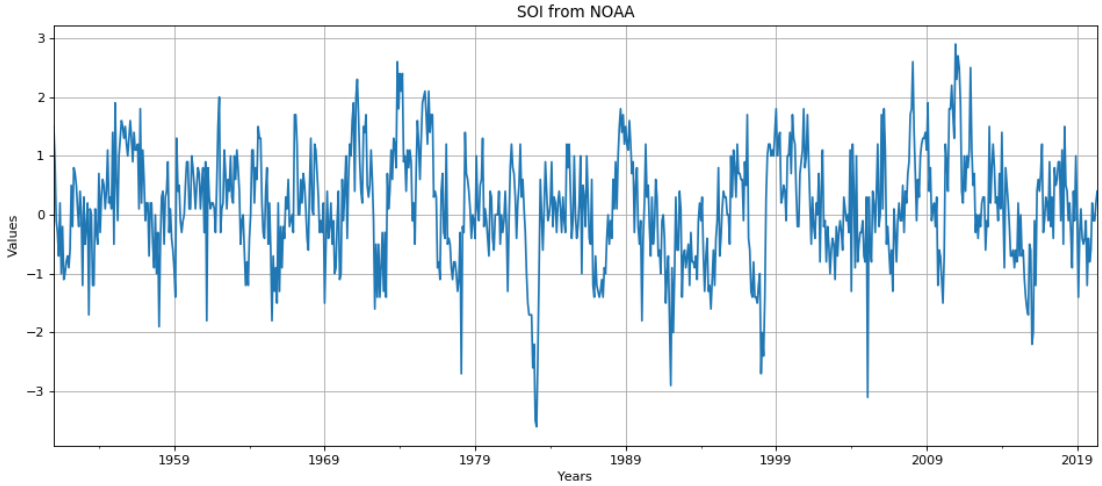

Figure S7. Time series of SOI index from NOAA, 1951–2019.

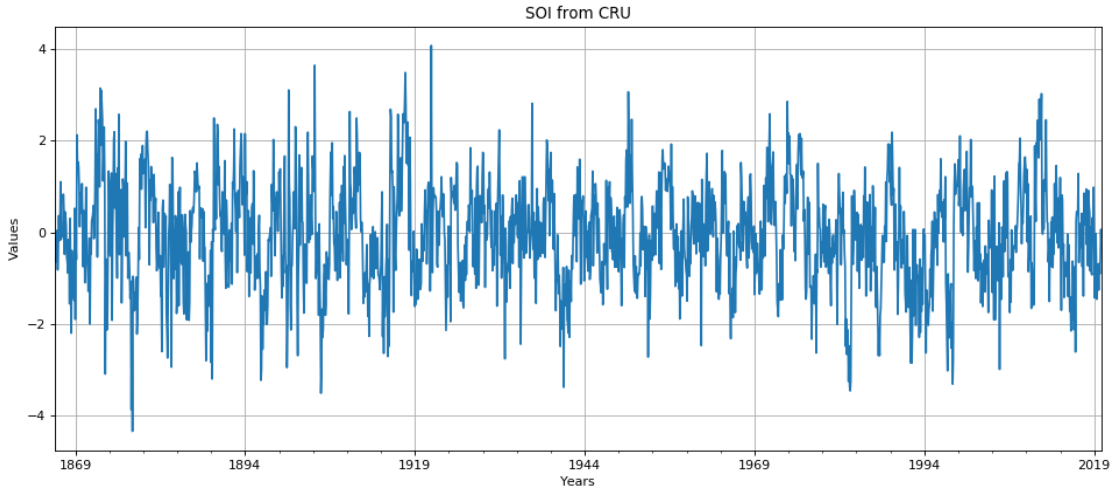

Figure S8. Time series of SOI index from CRU, 1860–2019.

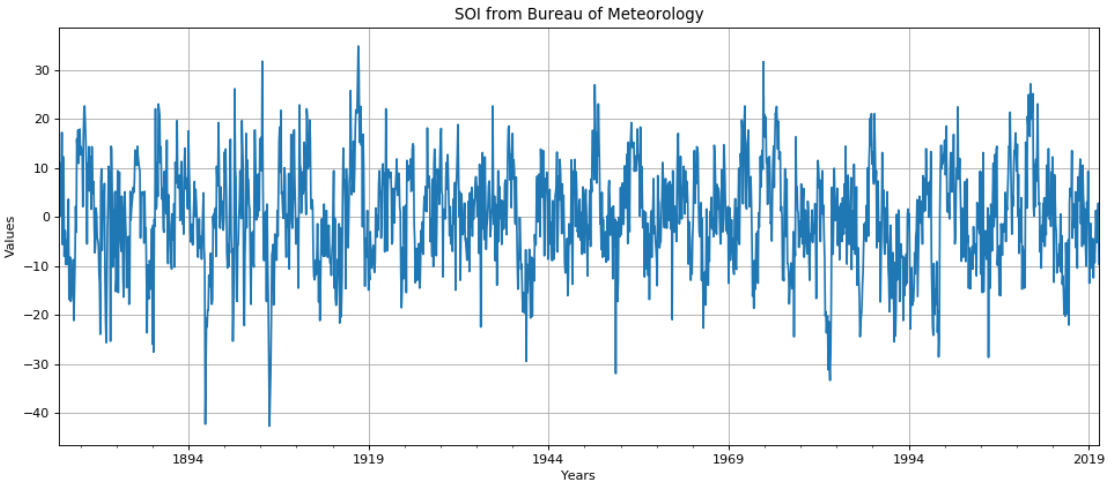

Figure S9. Time series of SOI index from Bureau of Meteorology, 1876–2019.

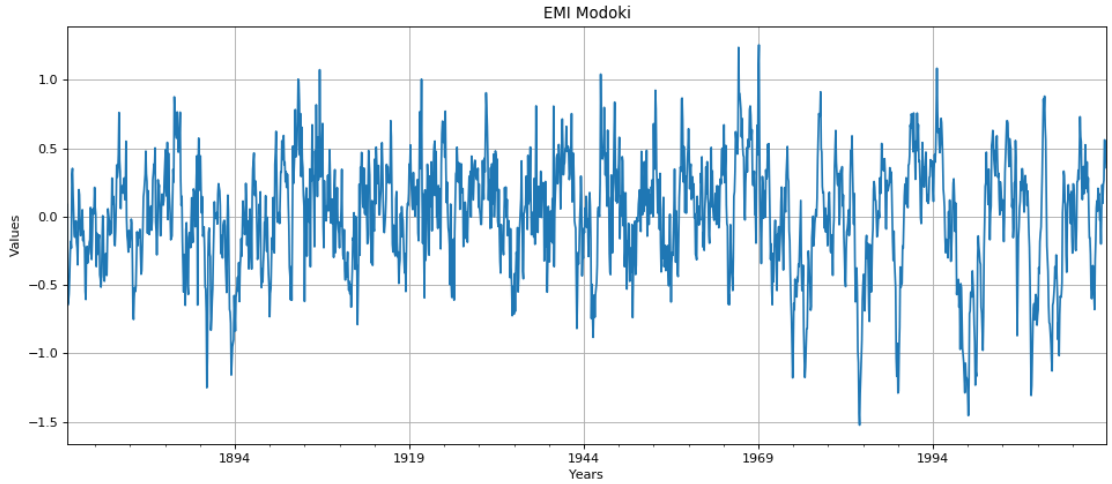

Figure S10. Time series of EMI Modoki, 1870–2018.

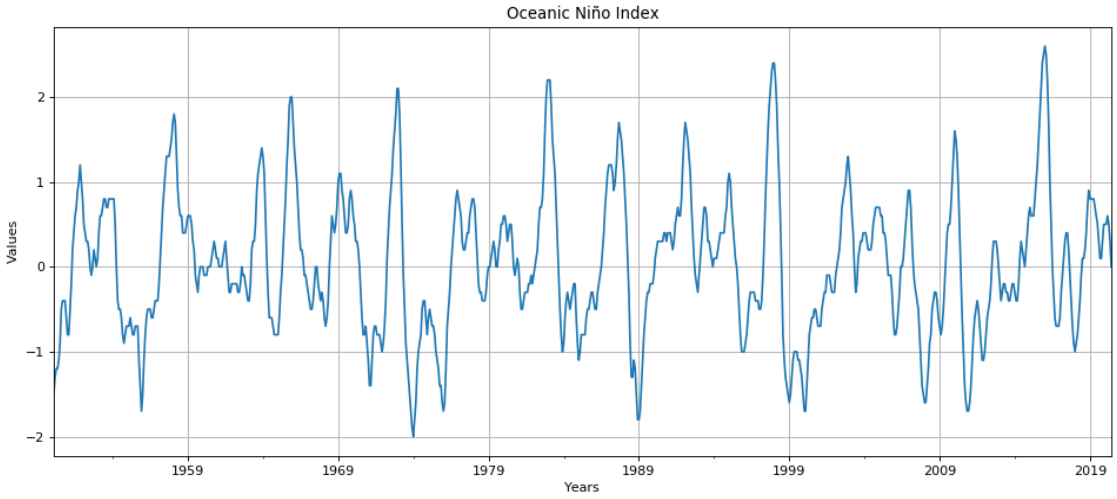

Figure S11. Time series of ONI, 1950–2019.

S3 Results of wavelet analysis of time series of ENSO indices (Nino and SOI indices)

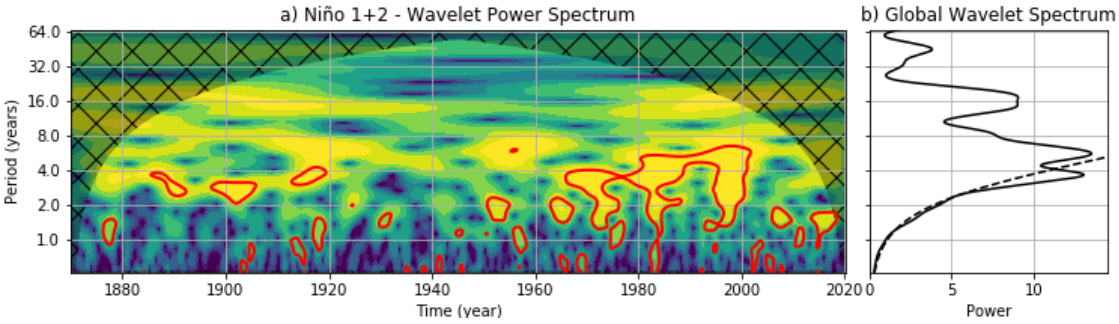

Figure S12. Results of wavelet analysis of the Niño 1 + 2 index, illustrating the quasi-periodic behaviour.

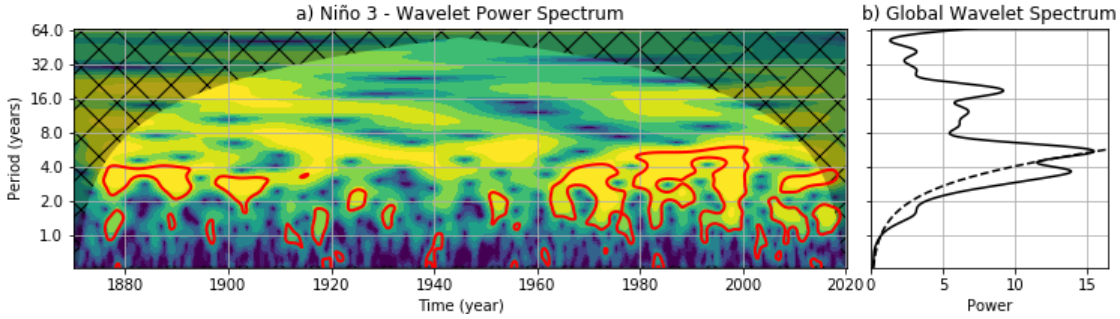

Figure S13. Results of wavelet analysis of the Niño 3 index, illustrating the quasi-periodic behaviour.

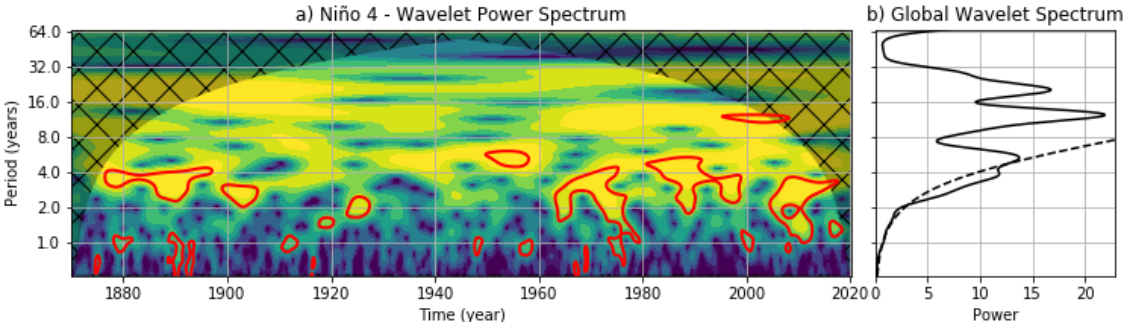

Figure S14. Results of wavelet analysis of the Niño 4 index, illustrating the quasi-periodic behaviour.

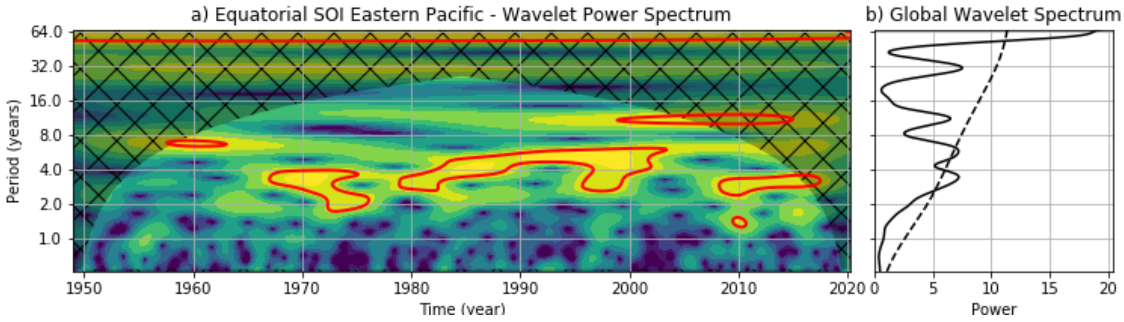

Figure S15. Results of wavelet analysis of the Equatorial SOI Eastern Pacific index, illustrating the quasi-periodic behaviour.

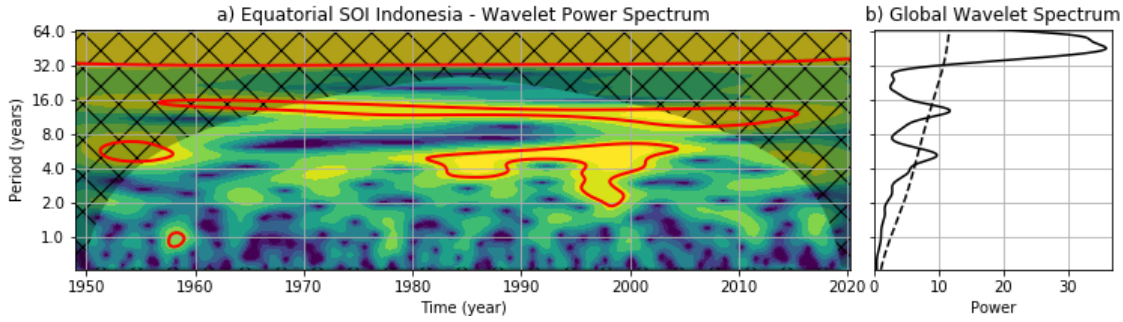

Figure S16. Results of wavelet analysis of the Equatorial SOI Indonesia index, illustrating the quasi-periodic behaviour.

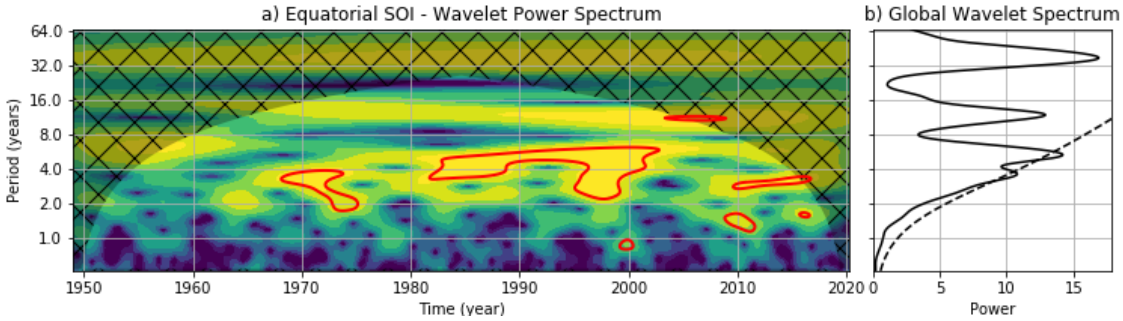

Figure S17. Results of wavelet analysis of the Equatorial SOI index, illustrating the quasi-periodic behaviour.

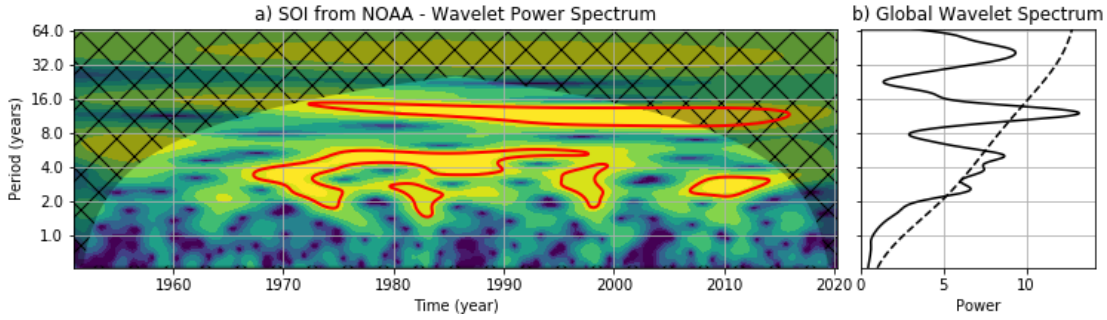

Figure S18. Results of wavelet analysis of the SOI index from NOAA, illustrating the quasi-periodic behaviour.

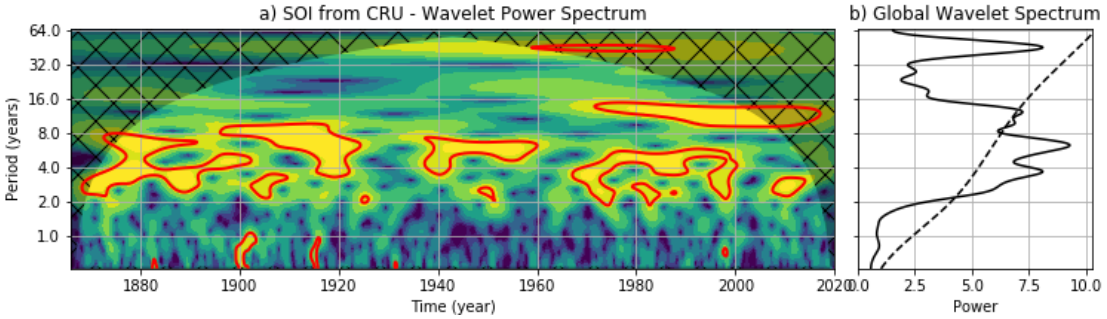

Figure S19. Results of wavelet analysis of the SOI index from CRU, illustrating the quasi-periodic behaviour.

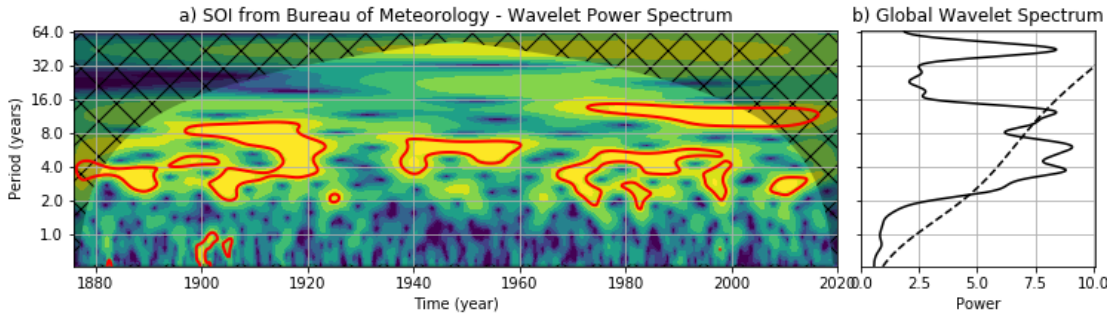

Figure S20. Results of wavelet analysis of the SOI index from Bureau of Meteorology, illustrating the quasi-periodic behaviour.

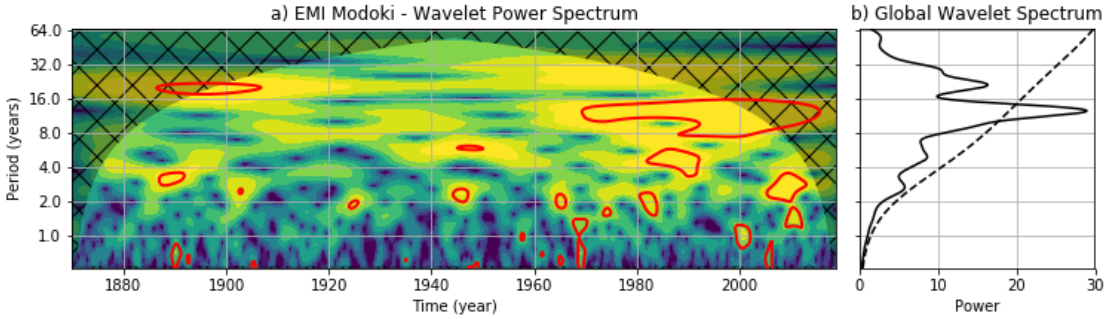

Figure S21. Results of wavelet analysis of the EMI Modoki index, illustrating the quasi-periodic behaviour.

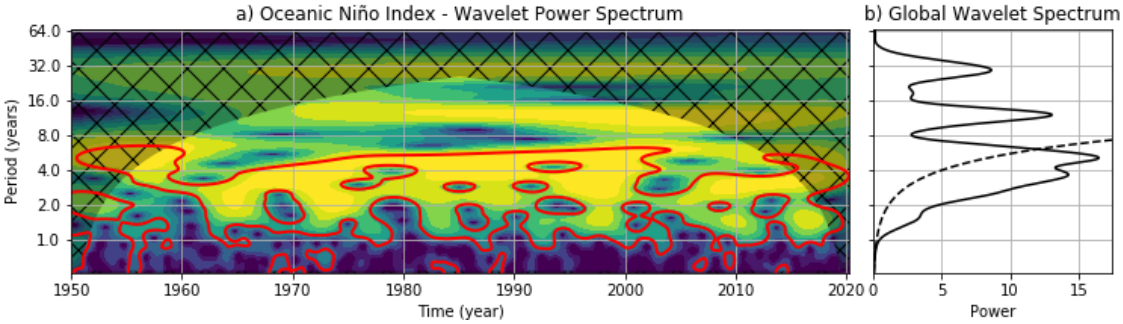

Figure S22. Results of wavelet analysis of the ONI index, illustrating the quasi-periodic behaviour.

S4 Time series of NAO indices

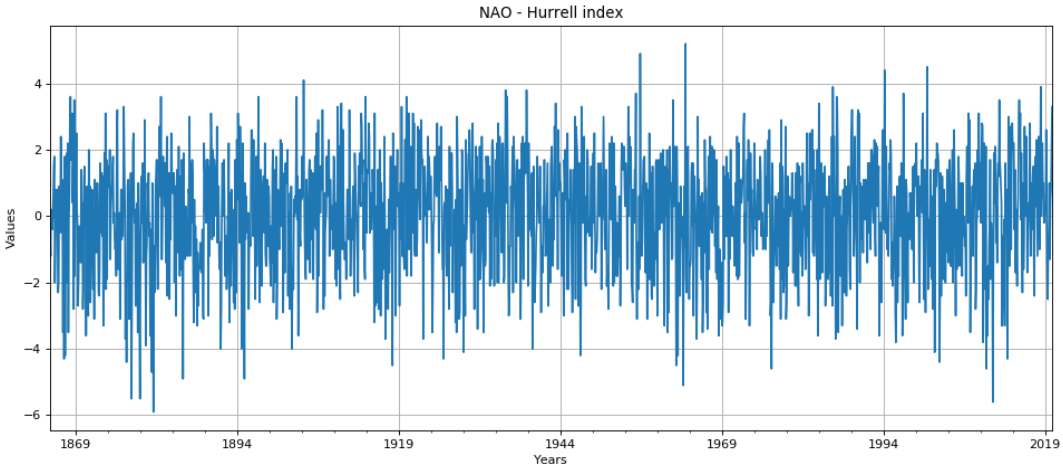

Figure S23. Time series of NAO - Hurrell index, 1865–2019.

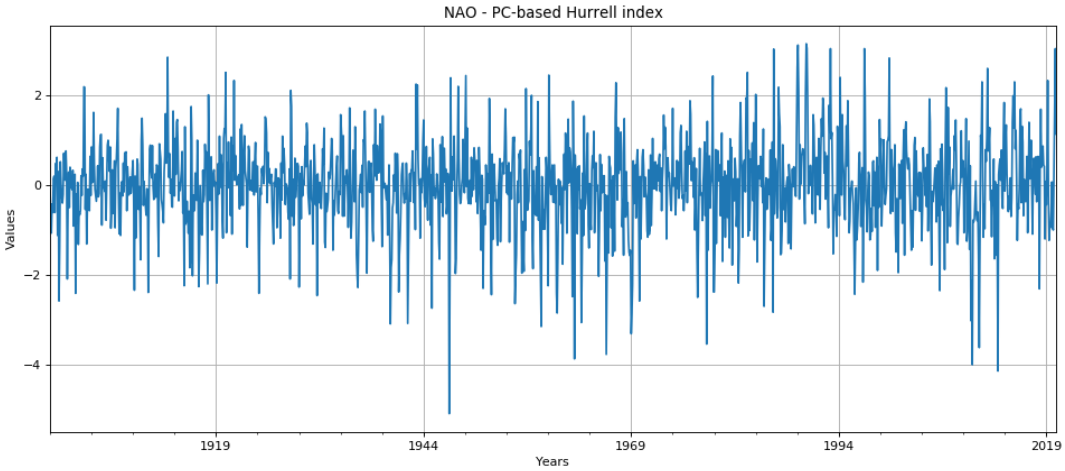

Figure S24. Time series of NAO – PC-based Hurell index,1880–2019.

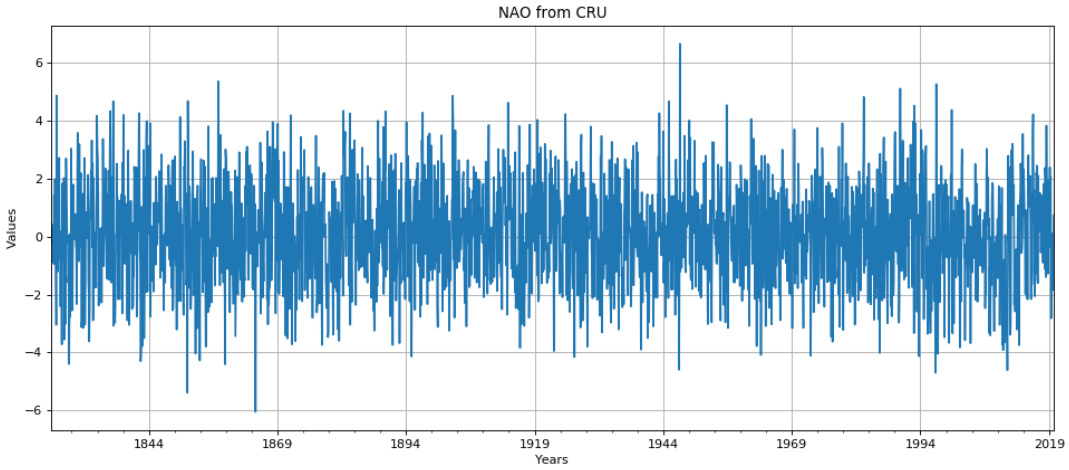

Figure S25. Time series of NAO index from CRU, 1865–2019.

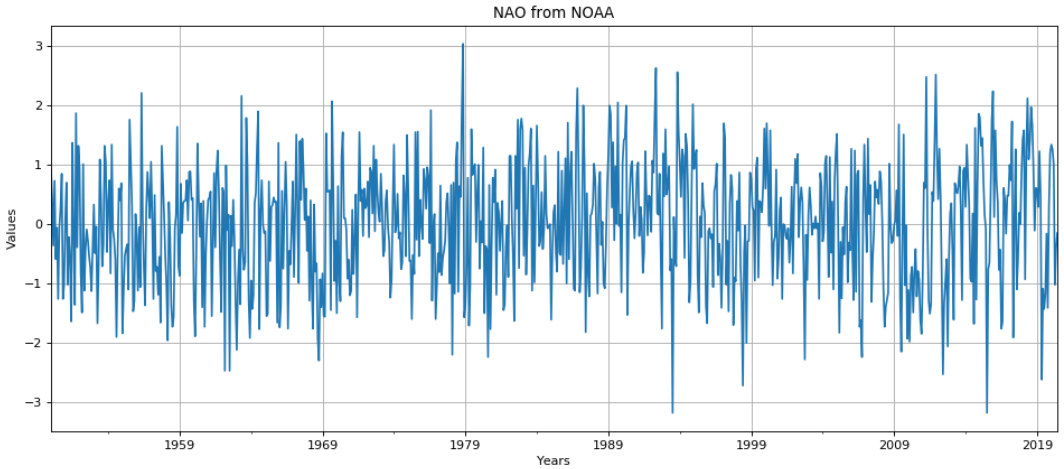

Figure S26. Time series of NAO index from NOAA, 1950–2019.

S5 Results of wavelet analysis of time series of NAO indices

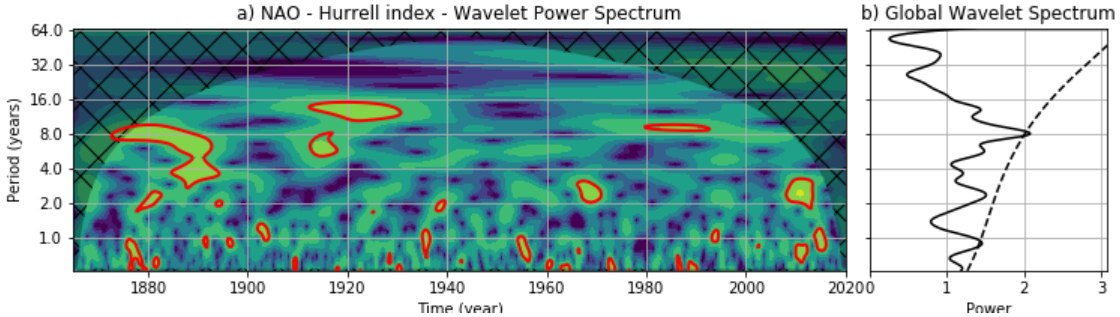

Figure S27. Results of wavelet analysis of the NAO - Hurrell index, illustrating the quasi-periodic behaviour.

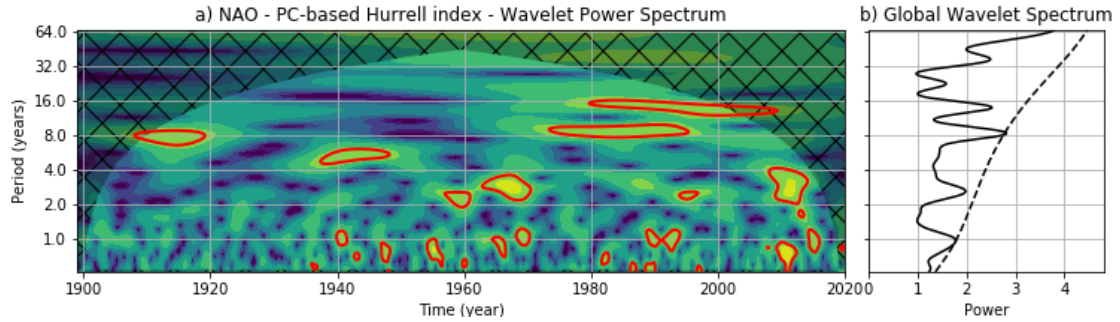

Figure S28. Results of wavelet analysis of the NAO – PC-based Hurrell index, illustrating the quasi-periodic behaviour.

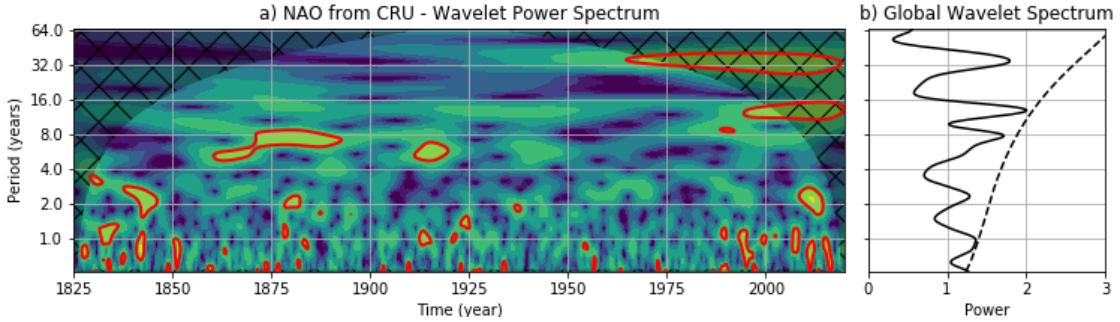

Figure S29. Results of wavelet analysis of the NAO index from CRU, illustrating the quasi-periodic behaviour.